Design of Probe to Investigate Energetic Electrons in Lower Hybrid Wave Plasmas in the TST-2 Spherical Tokamak*)

Kouji SHINOHARA, Osamu WATANABE, Akira EJIRI, Naoto TSUJII, Seowon JANG, Yi PENG, Kotaro IWASAKI, Yu-Ting LIN, Yongtae KO, Yuita SHIRASAWA, Taichi HIDANO, Yiming TIAN and Fumiya ADACHI

The University of Tokyo, Kashiwa, 277-8561, Japan

(Received 16 November 2022 / Accepted 5 January 2023)

The plasmas whose current is driven by the lower-hybrid wave (LHW) alone have been investigated on the TST-2 spherical tokamak. We are developing a probe to obtain the information about energetic electrons generated by the LHW. We investigated a detector, motivated by the lost fast-ion probe (LIP) or fast ion loss detector (FILD), which can identify the energy and pitch angle of captured ions. However, the pitch angle of electrons of interest is expected to be so small that it was found that a conventional configuration with the normal vector of an entrance-orifice surface almost perpendicular to the magnetic field line was not applicable. Thus, we accessed the feasibility of the configuration with two tiny orifices by which orbits, or the energy and pitch angle, of detected electrons can be well specified. We carried out numerical calculations by using calculation conditions and geometries which are manufacturable. The results suggest that it is difficult to identify the energy of detected electrons, but that it is possible to identify their pitch angle well. Based on the results, we designed the diagnostic system with 3 channels which will detect energetic electrons with the pitch angle of 3 - 5, 5 - 9, and 9.5 - 12.5 degrees, respectively.

Keywords: lower-hybrid wave, TST-2, spherical tokamak, energetic electron

DOI: 10.1585/pfr.18.2402006

1. Introduction

The performance of spherical tokamak (ST) benefits from a smaller aspect ratio [1]. To have a smaller aspect ratio, a machine without a center solenoid (CS) to induce a plasma current inductively is considered. We need to develop a method for a noninductive current drive to realize the machine without CS. The plasmas whose current is driven by the lower-hybrid wave (LHW) alone have been investigated on the TST-2 spherical tokamak [2] to investigate a better use of the LHW in ST [3–6]. The characteristics of the LHW plasma have been gradually revealed through comparisons between experiments and numerical simulations which can take into account wave-particle interactions. The results suggest that energetic electrons generated by the LHW play an important role in such plasmas. For example, it was reported that the equilibrium which is calculated by taking into account an anisotropic electron distribution can more fit to the electron density profile measured by a Thomson scattering diagnostics [7, 8]. In this calculation, the anisotropic electron distribution was modelled so as to approximate the phase-space distribution obtained by a numerical calculation of a wave-particle interaction [5]. In another example, observation results of hard X-rays suggest that many electrons strike a limiter wall in the low field side, namely that there are many electrons with a large orbit shift from a magnetic flux surface. This indicates electrons gain large energy from the LHW. The temporal behavior of the observation is recently reproduced qualitatively by a model calculation simulating the energy gain of electrons by the LHW and hard X-ray emissions from a limiter wall [9].

It is important to clarify the electron phase-space distribution by experimental measurements in order not only to validate the distribution modelled in the equilibrium calculation but also to investigate the basic process of the formation of the energetic electron distribution by the LHW. In addition, magnetic fluctuations with a fast frequency sweeping known as chirping in the range of MHz frequency are recently observed in a LHW plasma, which could tap a free energy from a gradient of a phase-space distribution. To investigate these interesting research topics, the measurement of the electron phase-space distribution is highly important.

The most plasma diagnostics measures the profile of a moment of the Maxwell distribution function, such as the density and temperature. The distribution can be represented only in terms of a space coordinate of the poloidal flux, ψ_p. However, the energetic electron distribution is not expressed by such a moment. We should investigate a phase-space distribution. The phase-space distribution is

author's e-mail: shinohara@k.u-tokyo.ac.jp

*) This article is based on the presentation at the 31st International Toki Conference on Plasma and Fusion Research (ITC31).

represented by the coordinate of (**r**, **v**) or by the reduced coordinate which consists of (P_φ, Λ, E) in an axisymetric system such as a tokamak, where the **r** indicates a real-space coordinate, the **v** a velocity coordinate, the P_φ the canonical toroidal angular momentum, the Λ the pitch parameter, and E the kinetic energy. Even, in the reduced coordinate, the distribution lies on the three-dimensional phase space. Thus, in general, it is hard to cover the whole phase space by a diagnostic system. In reality, we need to focus on a part of the phase space with a diagnostic system. By combining several diagnostics, we can obtain a wide range of the information on the distribution.

So far, the energetic electron distribution has been investigated by using X-rays induced by a bremsstrahlung mechanism in the TST-2 [10, 11]. The emission profile can give us the information on the energy distribution in a LHW plasma. However, the measured X-rays are probably contaminated by X-rays emitted by collisions of energetic electrons with components inside the vacuum vessel [9]. This fact motivates us to develop a new diagnostic system to clarify characteristics of energetic electrons which reach the components inside the vacuum vessel. Here, we report a fast electron probe under development which directly capture energetic electrons near the outer-limiter wall.

This paper is organized as follows. We investigate a feasible fast electron probe concept in section 2. Based on the feasibility study, we describe a configuration design to manufacture a system for measuring the pitch angle of energetic electrons in section 3. The summary is given in section 4.

2. Feasibility Study on Probe for Energetic Electron Measurement Induced by LHW

We investigate a feasible fast electron probe concept here.

The idea of the fast electron probe is from the scintillator-based lost fast-ion probe (LIP) or fast ion loss detector (FILD) as one of energetic ion diagnostics [12]. Figure 1 is a schematic drawing of the LIP. The LIP has an orifice. Energetic ions which enter from the orifice strike a screen on which a scintillator is painted. A positional relation between the orifice and the striking point can give us the information on a pitch angle and a Larmor radius since a charged particle undergoes a Larmor motion along a magnetic field line. Thus, the striking point suggests the pitch parameter, Λ, and energy, E, of the energetic ions at the probe position, which virtually indicates P_φ. The striking position can be measured as a scintillating position by capturing a two-dimensional image of the screen. In this way, the LIP can identify the property (P_φ, Λ, E) of the captured energetic ions or trace a temporal evolution of the number of the energetic ions with a specific (P_φ, Λ, E).

We can identify the property of energetic electrons if we can apply this method to the energetic electron mea-

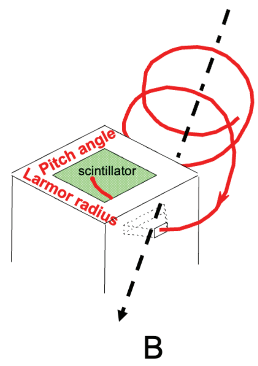

Fig. 1 Schematic drawing of the scintillator-based fast ion loss detector (LIP).

surement. But this method was not applied so far due to the following reason. This method utilized the characteristics that a charged particle undergoes a Larmor motion and can strike a screen which is apart from an orifice by a Larmor radius distance. Thus, to realize this method, the detected electrons should have a Larmor radius larger than about 5 mm in a realistic configuration. However, the electron mass is much lighter than the ion mass, which leads to a smaller Larmor radius by about 1/40 for a same perpendicular energy than that of a proton. Due to this, it is difficult to have an electron Larmor radius larger than 5 mm in conventional tokamaks with the toroidal filed of ∼1 T.

In the TST-2, we can have such a Larmor radius of larger than 5 mm for an electron since we can have stable LHW plasma discharges under a low toroidal field of less than 0.1 T. However, we soon noticed this is not a typical case in our LHW plasmas. Since LHW accelerates electrons in the direction parallel to the magnetic field, it is natural to assume that the typical pitch angle is small. We can predict two extreme cases. In the first case, we assume much short confinement time of fast electrons compared with its collision time because of orbit loss to wall limiters. Then, the distribution of electrons with the pitch angle larger than 0 is not changed, where the definition of the pitch angle is $\cos^{-1}(v_{//}/v)$. So, since $v_{//}/v_\perp \sim \sqrt{E_{fast}/T_e}$ where E_{fast} is tens keV and $T_e \sim 50$ eV, the pitch angle of observed fast electrons could be around 0 degrees. In the second case, we adopt the opposite assumption. We assume enough collision or good confinement without orbit loss. In this case, we can observe electrons with a finite pitch angle. The situation would be between these two cases. We assume the pitch angle is less than 10 degrees for this feasibility study.

This leads to the facts not only that the energetic electrons move almost parallel to the magnetic field line but also that they have small Larmor radii, which make this approach difficult as mentioned in the above. Figure 2 shows the dependence of the Larmor radius on the energy and pitch angle under the magnetic field strength of 0.05 T. In the calculation, the relativistic effect is taken into account.

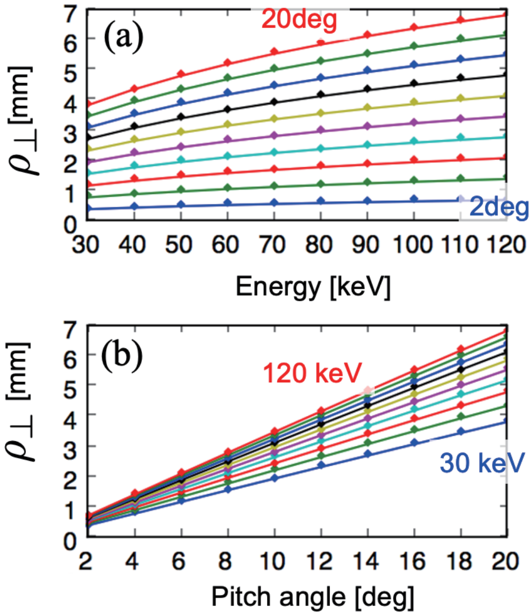

Fig. 2 Dependence of Larmor radius on energy and pitch angle at the position of the magnetic field strength of 0.05 T. (a) Horizontal axis is energy, and different curves are drawn with different pitch angles. Pitch angle varies from 2 degrees to 20 degrees with a 2-degree step from the bottom. (b) Horizontal axis is pitch angle, and different curves are drawn with different energies. Energy varies from 30 keV to 120 keV with a 10 keV step from the bottom.

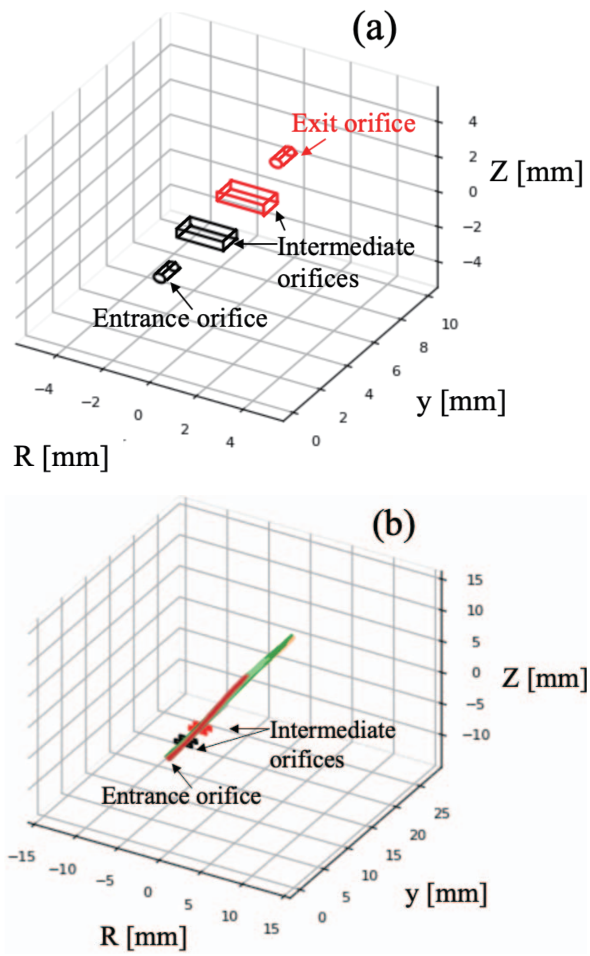

Fig. 3 Orifices to specify electron orbits. (b) Orbits specified by the orifices.

We can see that the Larmor radius is less than 3 mm when the pitch angle is less than 10 degrees even when the energy is larger than 50 keV and that the difference of the Larmor radius between 50 keV and 100 keV electrons is only by 1mm. We need to carry out a feasibility study under this condition.

Firstly, we assessed the feasibility of the conventional geometrical configuration with the normal vector of an entrance-orifice surface almost perpendicular to the magnetic field line as shown in Fig. 1. An actual probe needs to have a wall, which has the orifice, with a thickness of $>$ 0.5 mm and a scintillator plate with a thickness of $>$ 0.5 mm, then we found only electrons with the Larmor radius larger than 3 mm can reach a scintillator plate. The electrons of interest, whose pitch angle is less than 10 degrees, cannot satisfy such a condition for the Larmor radius. This also suggests the approach, in which the screen is utilized in the two-dimensional way as in the conventional LIP as shown in Fig. 1., is not possible for electrons with their pitch angle less than 15 degrees.

Thus, next, we studied the configuration with two tiny orifices which will select orbits with specific pitch angle and Larmor radius. In reality, the two tiny orifices are not two "points" but are two holes with a finite surface area. We evaluated the resolution on the pitch angle and Larmor radius by the orifices with a finite surface area. For this evaluation, we carried out numerical calculations with taking into account manufacturable size, geometry, a structure to reduce stray light, and so on. We want to minimize stray light, since the scintillation on the screen would not be bright compared with the visible light from a plasma. To realize the structure to reduce entering stray light from a plasma region into a scintillator, we placed additional two orifices in addition to two tiny orifices which specify orbits. Here, we call the orifice facing a plasma an entrance orifice, the orifice facing a scintillator an exit orifice, and the orifices between them intermediate orifices below. To be realistic, an orifice is not a point without a finite size. The entrance and exit orifices are holes with a cylinder shape and the intermediate orifices are holes with a right-rectangular-prism shape. In the calculation, we select orbits which pass through the inside of these holes and evaluate their pitch angle and energy. Figure 3 (a) shows a setup of these orifices as an example.

In the movement of an electron, the contribution of a magnetic drift on the screen is less than 1/100 mm since the trace time is around half the Larmor period, or less than 0.2 ns. Thus, we ignore the drift contribution in the calculation and utilized the simple gyromotion:

$$Z = \rho_\perp \sin(\Theta + \Theta_{ini}) + Z_{ini},$$

$$R = \rho_\perp(\cos(\Theta + \Theta_{ini}) - 1) + R_{ini},$$
$$Y = \rho_\parallel \Theta + Y_{ini}, \qquad (1)$$

where R is the major radius, Y is the coordinate along the magnetic field line, but the direction is opposite to the magnetic field. $e_Z = e_R \times e_Y$ where e_Z, e_R, e_Y are unit vectors for the Z, R, Y coordinate, respectively. Z can be the vertical direction when Y takes the pure toroidal direction in the counter-clockwise direction, but the direction of e_Y is not the pure toroidal direction since the poloidal field contribution in the magnetic field. Definitions of other values are as follows, the electron cyclotron frequency $\Omega_e \equiv eB/m_{er}$, the Larmor radius for the gyromotion $\rho_\perp \equiv v_\perp/\Omega_e$, the so-called parallel Larmor radius $\rho_\parallel \equiv v_\parallel/\Omega_e$, the gyrophase evolution by the gyromotion $\Theta \equiv \Omega_e t$. We take into account the relativistic effect for these values. The subscript "ini" in Eqs. (1) denotes that it is the value at the plasma-side surface of an entrance orifice.

About 100 thousand electrons with the following initial conditions are traced. Since the entrance surface of the entrance orifice has a finite surface area, electrons with various sets of (R_{ini}, Z_{ini}) are distributed on the entrance surface. The gyro-phase of an electron at the surface is distributed between $-\pi$ and π since it is not known in an actual experiment. The wide range of electrons are injected into the entrance orifice in order to identify the sensitivity to the energy and pitch angle for a specific orifice configuration. The energy ranges from 0 through 120 keV and the pitch-angle ranges from 0 through 24 degrees.

Figure 3 (b) depicts orbits which pass all the four orifices. The magnetic field strength is set to 0.1 T. The diameter and thickness of the entrance and exit orifices are $D = 0.5$ mm and $t = 1$ mm, respectively. The distance between the entrance and exit surfaces are 10 mm. The intermediate orifices are placed at the equally spaced position between them. The parameters to limit an orbit are the relative distance between the entrance and exit orifices in the direction of R and Z, $(\Delta R, \Delta Z)$. In this plot, $(\Delta R, \Delta Z) = (-0.2\text{ mm}, 0.5\text{ mm})$. We can see orbits are specified.

A scintillator screen is placed at R = −1 mm with its surface normal to the R direction since we need to capture the light emission from the air side with a positive R.

Figure 4 is two dimensional plots of orbits from the entrance orifice through the screen. Orifices and all orbits which pass the orifices are viewed from the R, Z, and Y direction in the plots (a), (b), and (c), respectively. In Fig. 5, several orbits selected from Fig. 4 are plotted, whose energy and pitch angle are limited to 50 keV and 4 degrees. The striking points on the screen are widely distributed. We can see that it is difficult to identify the energy and pitch angle of each orbit from the striking point on the screen since the distribution in Fig. 5 are comparable to that with electrons with a wide range of energy and pitch in Fig. 4.

The number distribution of electrons which pass

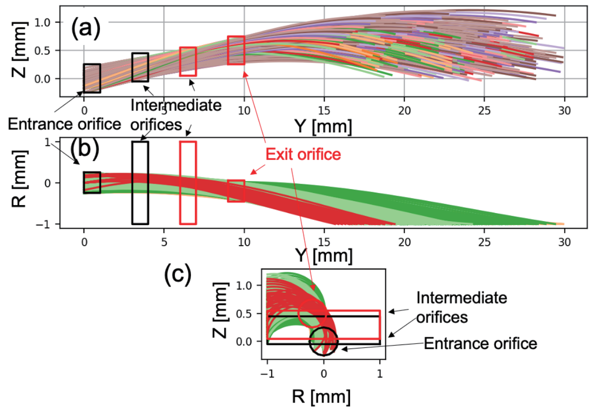

Fig. 4 Orifices and orbits specified by the orifices. (a) They are projected on YZ surface, (b) on YR surface, (b) on RZ surface.

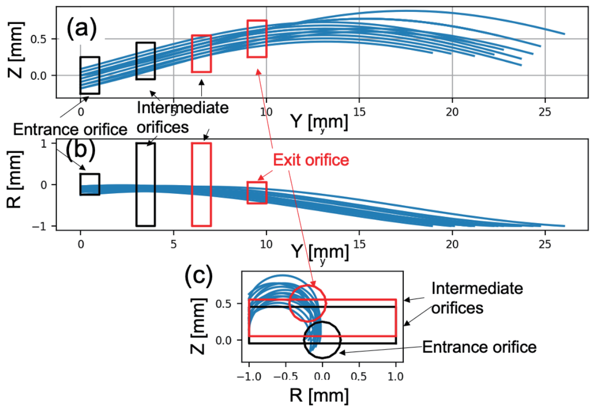

Fig. 5 Orbits specified by the orifices. Arranged in the same way as Fig. 4. In this case, the energy and pitch angle of injected electrons are 50 keV and 4 degrees.

through four orifices are plotted on the parameter plane of the injected energy and pitch angle in Fig. 6 (a). And the number distribution in Fig. 6 (a) was integrated over energy. The result is shown in Fig. 6 (b). These are for $(\Delta R, \Delta Z, D) = (-0.2\text{ mm}, 0.5\text{ mm } 0.5\text{ mm})$. Arranged in the same way, Figs. 6 (c) and (d) are for $(\Delta R, \Delta Z, D) = (-0.4\text{ mm}, 1.1\text{ mm}, 0.5\text{ mm})$, Figs. 6 (e) and (f) are for $(\Delta R, \Delta Z, D) = (-0.6\text{ mm}, 1.6\text{ mm}, 0.6\text{ mm})$. From these plots, we can see it is hard to obtain the information about the electron energy, though we also can see the energy cut-off around 40 keV for the configuration in Fig. 6 (a), and 10 keV for those in Figs. 6 (c) and (e). However, it is possible to measure the pitch angle with the resolution of about 4 degrees.

3. Configuration Design for Pitch Angle Measurement

Considering results in Section 2, we propose the method in which one channel consists of a set of entrance and exit orifices and captures energetic electrons with a

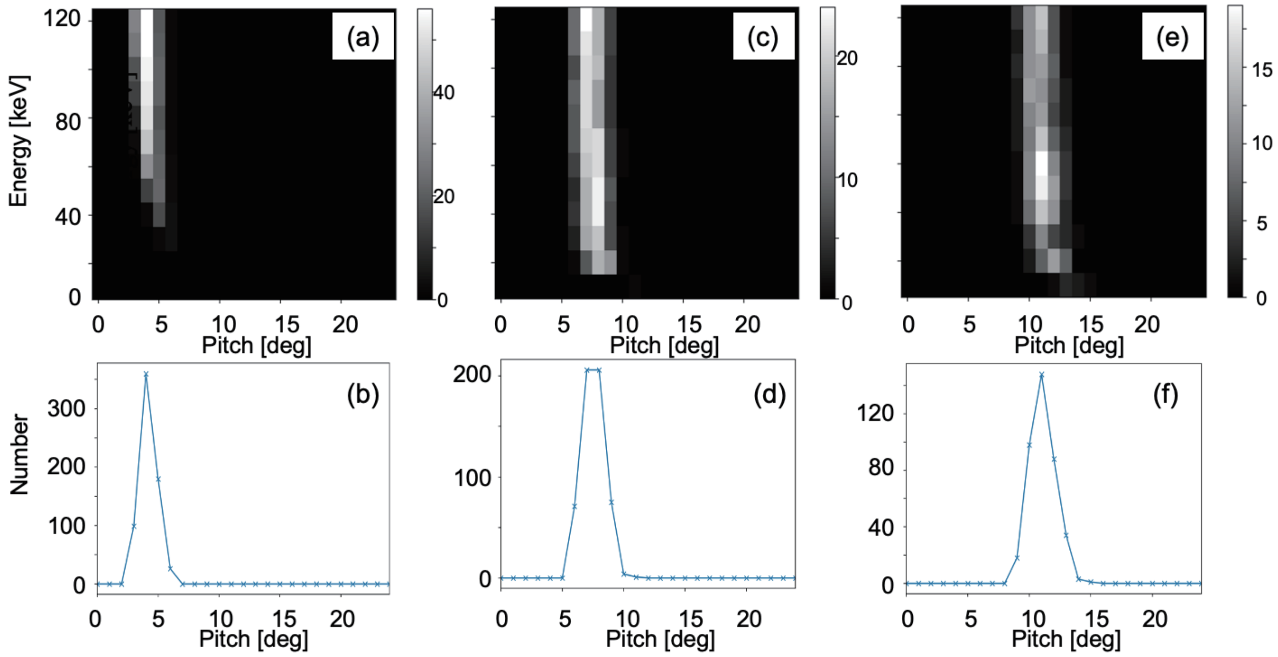

Fig. 6 (a), (c), (e) Distribution of particles which reached the scintillator screen on the plane spanned by pitch angle and energy. Its pitch angle dependence of the distribution for each is shown in (b), (d), and (f), respectively. (a) and (b) are the case for $(\Delta R, \Delta Z, D)$ = (−0.2 mm, 0.5 mm, 0.5 mm), (c) and (d) are for (−0.4 mm, 1.1 mm, 0.5 mm), (e) and (f) are for (−0.6 mm, 1.6 mm, 0.6 mm).

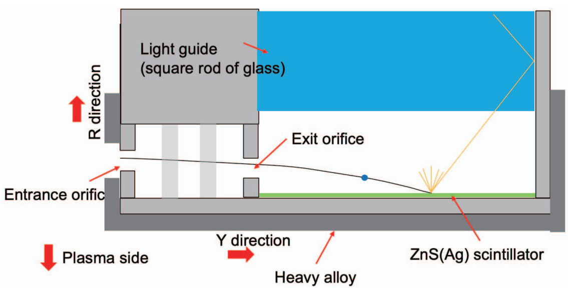

Fig. 7 Schematic drawing of a cross-section of one channel on the YR surface.

specific pitch angle as shown in Fig. 7 for a channel. Each channel has a separate cubicle enclosed by metal “side” walls. One of the side walls has an exit orifice. The scintillator plate is placed in its “bottom” side and its emission is measured from the “top” side. The bottom side corresponds to the plasma side and the top side to the air side. The emission does not go into other cubicle due to this cubicle structure. The strike position is not useful for electrons of interest. We measure the temporal evolution of emission intensity.

The most outer wall of the probe head which face to plasmas is made of a tungsten alloy, called heavy alloy, with high melting temperature.

We utilize a thin inorganic scintillator, ZnS(Ag). The thickness is about 10 micro m. The ZnS(Ag) emits a visible light with the wavelength of 450 nm and has been used for the screen of a cathode-ray tube (CRT) and so on. We confirmed this scintillator is effective for energetic electrons of interest by using the beta-ray source Ca-45 which can emit energetic electrons of up to 250 keV.

From the results in Section 2, e.g. as shown in Fig. 4, each channel needs the dimension of 30 mm length in the Y direction and of 3 mm width in the Z direction. Due to the limitation from the inner diameter of the vacuum interface on the TST-2, the number of channels is 3. The orifice parameters described in the caption in Fig. 6 are adopted as the configuration parameters. The target pitch angles are 3 - 5, 5 - 9, and 9.5 - 12.5 degrees, respectively.

In order to collect emissions efficiently, we utilized a transmission by using a light guide instead of an optical system by using a set of lenses. The light guide consists of a square rod of glass in the vacuum side and a square rod of acrylic resin in the atmosphere side. Their cross-section is 3×20 mm. An edge surface of the guide is placed just 6mm above the screen to have a wide solid angle, as shown in Fig. 7. The principle of the light guide is the same with the fiber optics, which utilizes a total reflection of its side wall.

We will have a vacuum window of 3 mm thickness between the glass rod and the acrylic rod. The surfaces of two rods face each other with the distance of about 3.2 mm. To avoid a cross talk with the nearest channel, we have a clearance of 4.5 mm between channels or nearest rods, taking into account the critical angle of about 42 degrees for the total reflection.

In this pitch angle measurement, the alignment in the Y direction, or the magnetic field direction is important.

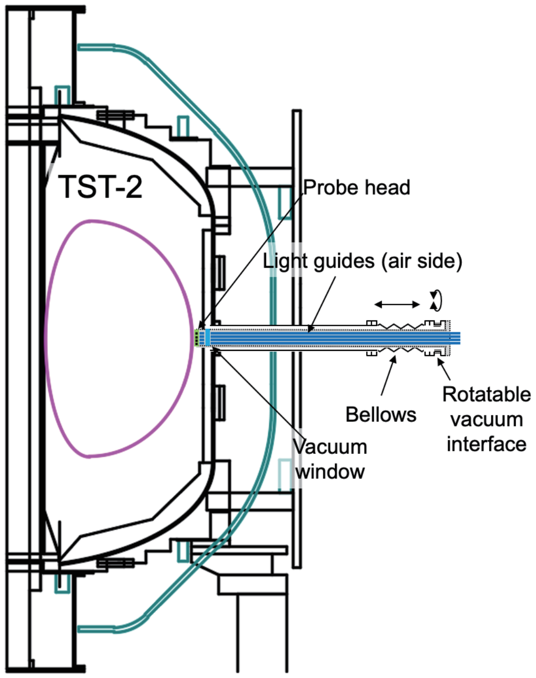

Fig. 8 Schematic drawing of an installation of energetic electron probe.

We will install a channel to detect particles which pass through two small-diameter orifices with the separation of 10 mm and the parameters of $(\Delta R, \Delta Z, D) = (0\,\mathrm{mm}, 0\,\mathrm{mm}, 0.08\,\mathrm{mm})$. We can carry out an alignment of the probe head with the accuracy of about 0.5 degrees by using this channel since the particle which can pass through these orifices have the pitch angle of less than 0.5 degrees or small energy.

The probe will be installed at the port on the midplane of the TST-2 as shown in Fig. 8. On the midplane, it is not difficult to keep the ratio of the radial component of the magnetic field strength B_r to the vertical component B_z less than 2% since the elongation of the TST-2 is large, kappa ~1.5. Thus, the alignment is virtually on the plane spanned by the toroidal and vertical directions. For this purpose, the probe will be installed using a rotatable vacuum interface. By using this mechanical feature and the channel with small-diameter orifices, it will be possible to carry out the alignment with accuracy of 0.5 degrees.

The probe will also have a mechanical feature which allows the head to move radially by using a vacuum bellows. Thus, the probe can capture electrons at various radial position or various P_φ. The feature will also help the probe head not to scrape plasmas or not to emit impurities by retracting the probe head when it is not in use.

We will utilize a photo multiplier tubes (PMTs) to detect photons transferred by a light guide. The PMT will be shielded by lead since the photoelectric surface of a PMT is sensitive to hard X-rays which are induced when energetic electrons strike a plasma limiter. The output signal from the PMT is fed into a current-to-voltage amplifier and the output of the amplifier will be digitized with high sampling rate for a pulse counting.

4. Summary

We are developing a probe to obtain the information on the energetic electron phase-space distribution in LHW plasmas in the TST-2. The energetic electrons are expected to have a pitch angle of around 0 degrees. We investigated a method to measure these electrons motivated by the LIP for energetic ions, which can identify the energy and pitch angle of captured ions. However, the pitch angle of electrons of interest is so small that it was found that a conventional configuration with the normal vector of an entrance-orifice surface almost perpendicular to the magnetic field line as shown in Fig. 1 was not applicable due to its small Larmor radius. Thus, we accessed the feasibility of the configuration with two tiny orifices, by which orbits of electrons to be detected can be specified. The energy and pitch angle of detected electrons can be determined if the orbits are well specified by the two orifices. We carried out numerical calculations for this assessment by using calculation conditions and geometries which are manufacturable or realistic. The results suggest that it is difficult to identify the energy of detected electrons, but that it is possible to identify their pitch angle. Based on the results, we designed the diagnostic system with 3 channels which will detect energetic electrons with the pitch angle of 3 - 5, 5 - 9, and 9.5 - 12.5 degrees, respectively. Now, we are manufacturing the system.

Acknowledgements

This work is supported by Grant-in-Aid for Scientific Research (C) (Grant No. 21K03506).

[1] Y.-K.M. Peng, Phys. Plasmas **7**, 1681 (2000).
[2] Y. Takase *et al.*, Nucl. Fusion **41**, 1543 (2001).
[3] Y. Takase *et al.*, Nucl. Fusion **51**, 063017(2011).
[4] T. Shinya *et al.*, Nucl. Fusion **55**, 073003(2015).
[5] N. Tsujii *et al.*, Nucl. Fusion **57**, 126032 (2017).
[6] S. Yajima *et al.*, Nucl. Fusion **59**, 066004 (2019).
[7] N. Tsujii *et al.* Plasma Fusion Res. **15**, 2402010 (2020).
[8] N. Tsujii *et al.* Nucl. Fusion **61**, 116047 (2021).
[9] A. Ejiri *et al.*, Plasma Fusion Res. **17**, 1402037 (2022).
[10] H. Togashi *et al.*, Plasma Fusion Res. **12**, 1402030 (2017).
[11] A. Ejiri *et al.*, Plasma Fusion Res. **15**, 1202023 (2020).
[12] S.J. Zweben *et al.*, Nucl. Fusion **29**, 825 (1989).